Invited paper Paolo TENTI, Alessandro COSTABEBER, Tommaso CALDOGNETTO, Paolo MATTAVELLI

University of Padova, Italy

Cooperative control of smart micro-grids based on conservative power commands

Abstract. *Smart micro-grids offer a new and wide application domain for power electronics. In fact, every distributed energy resource (DER) includes an electronic power processor (EPP) capable to control the active and reactive power flow from/to the distribution grid. If such EPPs perform cooperatively, they have the capability to fully exploit every local energy source while improving both power quality and distribution efficiency. This is of particular relevance in low-voltage residential micro-grids, where a plethora of small DERs may be active at the same time and the co-ordination of their operation can greatly improve the micro-grid performance. A simple and effective solution to achieve cooperative operation of EPPs is described in the paper. It makes use of a control method which requires power data exchange within the micro-grid and provides quasi-minimum distribution losses and local voltage support.*

Streszczenie. *Inteligentne mikro-sieci są obszarem nowych zastosowań energoelektroniki. Każde źródło rozproszonej energii (ang.: distributed energy resource - DER) zawiera procesor energoelektroniczny (ang.: electronic power processor – EPP) zdolny kontrolować przepływ mocy czynnej i mocy biernej ze źródła do sieci rozdzielczej i w kierunku odwrotnym. Jeśli EPP działają kooperatywnie mają wówczas zdolność pełnego wykorzystania każdego źródła, poprawiając jednocześnie jakość energii i sprawność jej rozdziału. Jest to szczególnie ważne w mikro-sieciach osiedlowych niskiego napięcia, w których może być jednocześnie czynnych wiele małych DER i koordynacja ich pracy może właściwości mikro-sieci znacząco poprawić. Niniejszy artykuł przedstawia proste i skuteczne rozwiązanie kooperatywnej współpracy EPP. Rozwiązanie to wykorzystuje metody sterowania, wymagające wymiany informacji wewnątrz mikro-sieci. Zapewnia ono niemal minimalne dystrybucyjne straty energii i lokalną kontrolę napięcia. (**Kooperacyjne sterowanie inteligentnych mikro-sieci oparte na kontroli mocy zachowawczej**)*

Keywords: Smart micro-grids; Distributed optimum control; Conservative power terms; Power quality; Distribution efficiency.
Słowa kluczowe: Inteligentne mikro-sieci, rozproszone sterowanie optymalne, moce zachowawcze, jakość energii, sprawność rozdzielcza.

Introduction

The increasing diffusion of renewable energy sources and energy storage devices connected to the distribution grid has the potential to progressively increase network efficiency, stability and flexibility [1-3]. For this aim each electronic power processor (EPP) interfacing a distributed energy resource (DER) with the distribution grid must be driven properly (controlling phase and shape of the injected currents so as to provide power flow regulation, reactive power control and local voltage stabilization), while preventing detrimental interference with other units. This can be achieved by supervisory control operated by a central dispatcher [4], but this solution appears not practical for residential micro-grids, where the distribution grid may host a plethora of small DERs, characterized by limited communication and data processing capability. In this case the control architecture must be flexible and scalable, so as to accommodate an increasing number of DERs and to automatically adapt to load variations and intermittent supply from renewable sources [5-7].

This paper extends the control approach presented in [8-10] and assumes that every EPP communicates, at low bit rate, with neighbor units. In spite of the simple communication and control infrastructure, the approach proposed here (surround control) provides full exploitation of renewable energy sources, proper utilization of energy storage elements, local voltage stabilization and minimum distribution losses. To show the effectiveness the proposed control, its performance is compared with that of an ideal optimum controller which, given the network parameters, determines the EPP currents that minimize the power loss in the entire micro-grid.

General control principles

In residential micro-grids, loads are fed by the mains at low voltage and the DERs contribute to power balance.

The general representation of a DER unit is shown in Fig.1.

It features an energy source ES (which may include a power generator and/or an energy storage device), and an electronic power processor EPP, which is normally made up of two conversion stages: the source-side converter (ac/dc or dc/dc stage), which interfaces the energy source with the dc link, and the line-side converter (single-phase or three-phase inverter), interfacing the dc link with the grid.
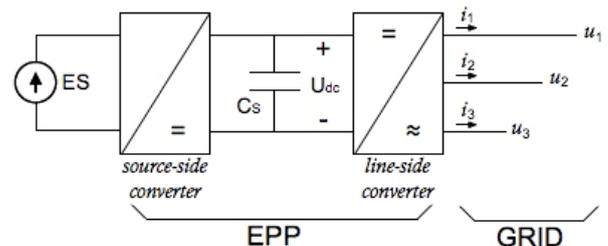

Fig. 1 - General structure of a distributed energy resource (DER) equipped with electronic power processor (EPP)

The control problem addressed in this paper relates with the need to operate cooperatively the EPPs, so as to improve the grid operation in terms of power loss on distribution lines. For this purpose, two operating modes must be considered.

In the *grid-connected operation mode*, the utility feeds part of the power consumed by the micro-grid and ensures voltage and frequency stabilization, as for traditional distribution grids. The function of the EPPs is to feed energy generated by the distributed sources to the grid and to supply active and reactive power as close as possible to the demanding loads, with the goal of reducing the distribution losses [11-13].

In the *islanded operation mode* the micro-grid performs autonomously, and load power consumption must be matched entirely by local generation units (PV panels, wind turbines, fuel cells, micro-turbines, batteries etc). Among the possible architectures for islanded microgrids, a master-slave approach is addressed here, being the solution that better fits the extension of the proposed loss minimization techniques to the islanded case. In that case, energy backup is provided by an auxiliary source, which intervenes when the utility goes off and becomes the main power supply of the micro-grid. The backup sources might be rated to feed a significant portion (say 30-50%) of total power demand, the remaining being met by DERs.

This paper deals with a simple control technique, which only requires narrowband communication between neighbor units and can be implemented in every EPP to ensure effective operation both in grid-connected and islanded mode. The emphasis of the paper is more on grid connected operation, the islanded operation will be only mentioned, and the details left to future developments of the work.

As a preliminary remark we observe that, in order to avoid network instability, EPPs should generally perform as controlled current sources. In this way, network dynamics are marginally affected even if the number of EPPs and their generated power change during the time. Moreover, there is no risk of current overshoots caused by voltage transients.

In practice, EPPs may operate as current sources only in the grid-connected mode, when the voltage is impressed by the mains [15]. In the islanded mode, one ore more EPPs can be required to perform as voltage sources, providing the voltage and frequency reference for micro-grid operation [16-17].

Another remark relates to the control instabilities which may occur due to the interaction of EPP control systems, which are coupled via the low impedances of power lines [18]. These instabilities can be avoided either by adopting a distributed concurrent control architecture or by assuming that the EPPs adjust sequentially their control parameters, thus avoiding simultaneous actions of the controllers. The first technique is more complex and ensures better dynamic performance; the second is simpler but provides slower response. In spite of their different operation, both techniques can implement the control principles described in this paper.

Optimum micro-grid control: minimization of total distribution losses

This section investigates the optimum control with the final objective of minimizing the distribution losses. This maximizes the hosting capacity of the micro-grid and also stabilizes the grid voltages. In fact, the distribution losses are minimized when the loads are fed by neighbor power sources, so that the active and reactive current flow across the distribution lines reduces and the voltage drops on the line impedances reduce too. For these peculiarities, the optimum control performance can be regarded as a benchmark for any other control techniques. As it will be shown, the optimum control require a full knowledge on the microgrid, including topology, cables, loads and generators, and therefore can be regarded as a theoretical ideal case for loss minimization.

Consider a micro-grid fed by the mains at the Point of Common Coupling (PCC) and let 0 be the PCC node. If we assume a *tree-shaped grid* the number N of grid nodes (excluding node 0) coincides with the number of distribution paths (grid branches). Thus, the incidence matrix $\underline{A}$ of the network (which describes the network topology by giving, in its rows, the starting and ending node of all branches) is squared and invertible.

Assuming for simplicity that the grid voltages and currents are purely sinusoidal, they can be represented by phasors [19]. Let $\dot{\underline{J}}$ be the vector of branch currents and $\dot{\underline{I}}$ be the vector of node currents (loads and EPPs), the Kirchhoff's equations at the grid nodes can be expressed in the form:

(1.a) $\quad \dot{\underline{I}} = \underline{A}^T \dot{\underline{J}}$

where index T means transpose. By inversion we get:

(1.b) $\quad \dot{\underline{J}} = \left(\underline{A}^T \right)^{-1} \dot{\underline{I}}$

The distribution losses are generally expressed by:

(2) $\quad P_d = \dot{\underline{J}}^T \underline{R} \dot{\underline{J}}^*$

where index * means complex conjugate and $\underline{R}$ is the diagonal matrix of branch resistances. Owing to (1.b) the losses can also be expressed as a function of the load currents by:

(3.a) $\quad P_d = \dot{\underline{I}}^T \underline{B} \, \dot{\underline{I}}^*$

where:

(3.b) $\quad \underline{B} = \underline{A}^{-1} \underline{R} \left(\underline{A}^{-1} \right)^T$

Note that, by definition, matrix $\underline{B}$ is symmetrical and function P_d is real.

The computation is more complex in case of *meshed grids*, where the incidence matrix is not invertible. Even in this case, however, equation (3.a) holds and the optimum control approach described hereafter remains valid.

Let $\dot{\underline{I}}_a$ be the currents fed by the EPPs into *active nodes* and $\dot{\underline{I}}_p$ be the currents absorbed by the loads at *passive nodes*, Eq.3.a can be partitioned in the form:

(4.a) $\quad P_d = \begin{vmatrix} -\dot{\underline{I}}_a^T & \dot{\underline{I}}_p^T \end{vmatrix} \begin{vmatrix} \underline{B}_{a,a} & \underline{B}_{a,p} \\ \underline{B}_{p,a} & \underline{B}_{p,p} \end{vmatrix} \begin{vmatrix} -\dot{\underline{I}}_a^* \\ \dot{\underline{I}}_p^* \end{vmatrix}$

which can be rewritten as:

(4.b) $\quad P_d = \dot{\underline{I}}_a^T \underline{B}_{a,a} \dot{\underline{I}}_a^* - 2\Re\left(\dot{\underline{I}}_a^T \underline{B}_{a,p} \dot{\underline{I}}_p^* \right) + \dot{\underline{I}}_p^T \underline{B}_{p,p} \dot{\underline{I}}_p^*$

where $\Re$ indicates the real part of the argument. Optimum EPP currents result by assuming $\dfrac{\partial P_d}{\partial \dot{\underline{I}}_a} = 0$, which gives:

(5) $\quad \dot{\underline{I}}_a = \underline{B}_{a,a}^{-1} \underline{B}_{a,p} \dot{\underline{I}}_p$

Eq.5 sets the theoretical basis for optimum control of distributed EPPs, since it gives the optimum EPP currents as a function of grid parameters and load demand.

The approach can be extended to entail also the boundaries set by the EPP current limits and by the islanded operation, which requires zeroing of the current at node 0.

Note finally that (5) is separately valid for the real and imaginary part of the currents, thus allowing for independent control of active and reactive power.

From the application point of view we observe that:
- Applying the optimum control technique expressed by (5) requires the knowledge of the network topology and parameters, which is reasonable for medium-voltage distribution grids but may be difficult for low-voltage residential micro-grids.
- The optimum control approach is well suited if all data are managed by a central control hub, while it is difficult to apply in presence of a distributed control environment, which is typical of smart micro-grids.
- The EPP active currents are usually constrained by the power generated by the local energy sources. However, optimum control can profitably be applied to reactive currents, which are only limited by the VA ratings of the EPPs.

Quasi-optimum micro-grid control: Minimization of local distribution Losses

Considering the case where the knowledge required by the optimum control is not available, different quasi-optimum techniques can be implemented in order to approach the ideal case. All of them rely on limited knowledge of the network and on a sequence of control action taken using the partial available information and

taking advantage of ICT technology. The distribution losses of the micro-grid can locally be minimized if the voltages and currents impressed at the active grid nodes follow the control principles discussed in [8,10] and summarized hereafter.

A. Loss minimization in distribution paths

Fig.2 shows a simplified single-phase representation of a distribution path connecting two neighbor active nodes A and B. Assuming that node voltages and currents are sinusoidal, we refer to node voltage phasors $\dot{U}_A$ and $\dot{U}_B$. Similarly, $\dot{I}_{AB}$ and $\dot{I}_{BA}$ represent the phasors of the currents fed by nodes A and B into path A-B.
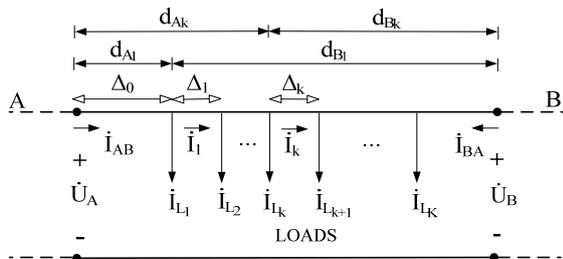

Fig. 2 – Representation of the distribution line between two active nodes A and B

Let $\dot{I}_{Lk}$ be the current absorbed by the k-th load connected along path A-B, Δ_k the distance between loads k and $k+1$, and $\dot{I}_k$ the line current flowing in branch Δ_k, we have:

$$(6) \qquad \dot{I}_k = \dot{I}_{AB} - \sum_{\ell=1}^{k} \dot{I}_{L\ell}$$

The power loss in path A-B is given by:

$$(7) \qquad P_{loss} = \sum_{k=0}^{K} r \Delta_k I_k^2$$

where r is the resistance per unit of length of the distribution line. It can be shown that the power loss is minimized if $\dot{U}_A = \dot{U}_B$. Correspondingly, currents $\dot{I}_{AB}$ and $\dot{I}_{BA}$ take the optimum values:

$$(8) \qquad \begin{cases} \dot{I}_{AB}^{opt} = \dfrac{1}{d_{AB}} \sum_{k=1}^{K} \dot{I}_{Lk} d_{Bk} \\ \dot{I}_{BA}^{opt} = \dfrac{1}{d_{AB}} \sum_{k=1}^{K} \dot{I}_{Lk} d_{Ak} \end{cases}$$

where d_{AB} is the path length, and d_{Ak} [d_{Bk}] is the distance between load k and node A [B]. Equation (8) shows that in case of constant section of the distribution cables (the case where the resistances per unit of length can be replaced by the distances), the optimum currents demanded to the active nodes depend only on the load distribution along path A-B.

Instead, if $\dot{U}_A \neq \dot{U}_B$ a circulation current appears and the currents fed by nodes A and B become:

$$(9) \qquad \begin{cases} \dot{I}_{AB} = \dot{I}_{AB}^{opt} + \dfrac{\dot{U}_A - \dot{U}_B}{\dot{z}\, d_{AB}} = \dot{I}_{AB}^{opt} + \dot{I}_{AB}^{circ} \\ \dot{I}_{BA} = \dot{I}_{BA}^{opt} + \dfrac{\dot{U}_B - \dot{U}_A}{\dot{z}\, d_{AB}} = \dot{I}_{BA}^{opt} + \dot{I}_{BA}^{circ} \end{cases}$$

By working out equations (8) and (9), the power loss in path A-B can be expressed in the simple form:

$$(10) \qquad P_{loss} = P_{loss}^{opt} + R_{AB}\, I_{AB}^{circ\,2} = P_{loss}^{opt} + R_{AB} \left| \frac{\dot{U}_A - \dot{U}_B}{\dot{Z}_{AB}} \right|^2$$

where $\dot{Z}_{AB} = R_{AB} + j X_{AB}$ is the impedance of path A-B.

The first addendum of (10) corresponds to the minimum distribution losses, which occur in the optimum condition (8) and depend only on the load currents and their distribution along path A-B. The second addendum pertains to the circulation currents and depends on the voltage difference between nodes A and B. Equation (10) confirms that the minimum distribution losses occur when $\dot{U}_A = \dot{U}_B$ and the circulation current vanishes.
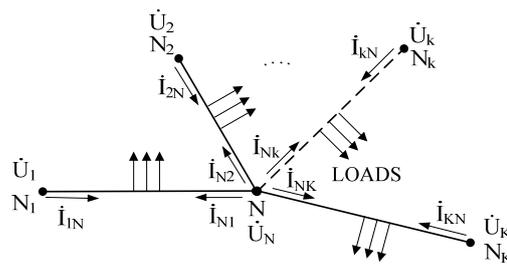

Fig. 3 – Representation of a grid section converging in node N

Optimum node voltages

Consider now a radial section of a micro-grid, sketched in Fig.3, where active node *N* links to surrounding active nodes $N_1 \ldots N_K$ through distribution paths $L_1 \ldots L_K$.

Let $\dot{U}_N$ be the voltage of node *N*, and $\dot{U}_k$ $(k=1 \ldots K)$ those of surrounding nodes, from (9) we get the value of the general current injected at node N (and not necessarily the current corresponding to loss minimization) by simply adding all terms corresponding to paths $L_1 \ldots L_K$:

$$(11) \qquad \dot{I}_N = \sum_{k=1}^{K} \dot{I}_{Nk} = \underbrace{\sum_{k=1}^{K} \dot{I}_{Nk}^{opt}}_{\dot{I}_N^{opt}} + \underbrace{\sum_{k=1}^{K} \frac{\dot{U}_N - \dot{U}_k}{\dot{Z}_k}}_{\dot{I}_N^{circ}} = \dot{I}_N^{opt} + \dot{I}_N^{circ}$$

where $\dot{Z}_k = R_k + j X_k$ are the path impedances and Z_k the corresponding module. Optimum current $\dot{I}_N^{opt}$ depends on the loads distribution along paths $L_1 \ldots L_K$, according to (8), while total circulation current $\dot{I}_N^{circ}$ depends on the voltage differences between node *N* and the surrounding nodes. By extending (10) we derive the total distribution loss in paths $L_1 \ldots L_K$ in the form:

$$(12) \qquad P_{loss}^{tot} = \sum_{k=1}^{K} P_{k\,loss}^{opt} + \sum_{k=1}^{K} R_k \frac{\left| \dot{U}_N - \dot{U}_k \right|^2}{Z_k^2}$$

This local distribution loss is minimized if the second term in (12) vanishes, and therefore if voltage $\dot{U}_N$ takes the value:

$$(13.a) \qquad \dot{U}_N^{opt} = \sum_{k=1}^{K} \frac{R_k}{Z_k^2} \dot{U}_k \left/ \sum_{k=1}^{K} \frac{R_k}{Z_k^2} \right.$$

Recalling that all the distribution paths $L_1...L_K$ have the same impedance per unit of length, equation (13.a) simplifies in the form:

$$(13.b) \quad \dot{U}_N^{opt} = \sum_{k=1}^{K} \frac{\dot{U}_k}{d_k} \Bigg/ \sum_{k=1}^{K} \frac{1}{d_k}$$

where d_k are the lengths of paths $L_1...L_K$.

Eqs.13 give the value of node voltage $\dot{U}_N$ which minimizes the local distribution loss and set therefore the basis for quasi-optimum control. In fact, each EPP can compute its voltage reference by (13), provided that the parameters of distribution paths are given and that the surrounding node voltages are known by infra-node communication.

Clearly, the result is not fully optimized since the local optimization procedure (11)-(13) implicitly assumes that the voltages of the surrounding nodes are impressed by voltage sources. In practice, the surrounding node voltages depend also on the voltage at node N since the EPPs are driven as current sources, whose current references are derived from (13) by applying the Thevenin equivalent. Despite this approximation, by iterating the quasi-optimum local control algorithm among all EPPs, the optimum operating condition is approached. Compared to the optimum control technique presented in section III, this method has some advantages:

- It requires only local knowledge of network topology and parameters; in a first approximation, controlling an active node requires only to know the neighbor nodes and their distance.
- It fits well with distributed control, since each active node performs independently and needs to communicate with neighbor nodes only.

Note also that minimizing the local distribution losses means that each load is fed by the power sources nearby. Thus, quasi-optimum control behaves similarly to optimum control, and local voltage stabilization is ensured also in this case.

The control methods based on this principle are named *voltage-based controls* .

B. Optimum node currents

In smart micro-grids, each load of Fig.2 may be equipped by a smart meter, capable to measure the load current and to send this information around. Thus, optimum node current $\dot{I}_N^{opt}$ can be derived, according to (8), by simply adding the current demands of all surrounding loads fed by paths $L_1...L_K$. This requires to know the distances between active node N and the surrounding passive nodes, but gives an alternative method to establish directly the optimum current references of the active nodes.

The control methods based on this principle are called *current-based controls.*

Of course, applying current-based control requires a pervasive communication system, connecting every node in the micro-grid. Instead, voltage-based control performs independently of load currents, and requires to sense only the voltages at the active nodes.

On the other hand, voltage-based control is more sensitive to parameter variations and computation errors, since even small inaccuracies in the calculation of the voltage references can cause large circulation currents in the distribution paths. Instead, current-based control is inherently robust against parameter variations and control inaccuracy.

Surround Control

Equations (8) and (13) set the basis for distributed control of the micro-grid according to the *surround* technique [8]. In fact each EPP can be controlled to feed the optimum current or to drive its node voltage as close as possible to the optimum value. For this aim, however, each EPP must communicate with neighbor nodes.

In order to implement surround control we need, first of all, to identify the active nodes in the micro-grid. In residential settlements, active nodes physically coincide with the power meters of each prosumer (customer equipped with energy sources or energy storage capability). Furthermore, it is required that:
1. active nodes implement narrowband communication, e.g., by Powerline Communication protocols [20];
2. the communication infrastructure ensures the needed accuracy and security of data, and sufficient bandwidth to allow synchronization of voltage and current phasors [19];
3. the map of active nodes and their distances is updated at the time of installation of each new active node (given the distribution grid layout), or is dynamically adjusted by ranging techniques [21].

Correspondingly, each active node N cyclically addresses an inquiry to neighbor active nodes, which return their voltage phasors. The local controller then computes the voltage reference according to (13) and feeds this signal to the EPP.

The surround control technique performs well, however it is affected by severe implementation problems. In fact, the identification of neighbor nodes and the node-to-node communication require a sophisticated communication infrastructure. Moreover, the control is based on voltage or current phasors, i.e., it requires precise measurements and synchronization in all nodes of the micro-grid, since even small errors in the voltage phase or amplitude can affect control performance. For these reasons, hereafter we discuss a different control technique, which does not require to know grid topology but node-to-node distances. Further, it relies on power commands, which do not require precise synchronization of control actions in the micro-grid nodes. This control method is called cooperative control and is describes hereafter.

Cooperative control

The distributed cooperative control technique proposed here approaches the optimization problem from a simplified and more intuitive perspective. We observe that the distribution losses tend to reduce if each DER supplies only the active and reactive power demanded by the loads nearby. More generally, we may assume that each active node contributes to the power demanded by the passive nodes in inverse proportion to their distance. This simplified approach, which does not require to know grid topology nor grid parameters, but node-to-node distances, leads to a quasi-optimum operating condition characterized by low distribution losses and good stabilization of voltage profiles. Moreover, it can be emended to account for the limited power capability of the EPPs connected to active grid nodes.

The distributed cooperative control performs as follows. Let $\dot{S}_m$ be the complex power absorbed by the load tied at generic passive grid node m ($m = 1...M$) and $\dot{S}_n$ be the complex power fed to the grid by the EPP connected at generic active node n ($n = 1...N$):

$$(14) \quad \dot{S}_m = P_m + jQ_m \quad , \qquad \dot{S}_n = P_n + jQ_n$$

In principle, the cooperative control shares the power demand $\dot{S}_m$ of each passive node among all active nodes n (including the utility at PCC) in inverse proportion to their

distance d_m^n from node m. Accordingly, the complex power $\dot{S}_m^n$ requested from passive node m to active node n is:

$$(15.a) \quad \dot{S}_m^n = \dot{S}_m \frac{1}{d_m^n} \left(\sum_{n=1}^{N} 1/d_m^n \right)^{-1}$$

The total power requested to active node n becomes:

$$(15.b) \quad \dot{S}_n = \sum_{m=1}^{M} \dot{S}_m^n = P_n + jQ_n$$

In practice, this power request can exceed the actual power capability of node n. Thus, the distance-based sharing criterion (15) must be emended to comply with the actual power capability of active nodes. For this purpose, (15.a) can be rewritten in the form:

$$(16) \quad \begin{aligned} \dot{S}_m^n &= P_m^n + jQ_m^n = \\ &= P_m \frac{\beta_{nP}}{d_m^n} \left(\sum_{n=0}^{N} \frac{\beta_{nP}}{d_m^n} \right)^{-1} + jQ_m \frac{\beta_{nQ}}{d_m^n} \left(\sum_{n=0}^{N} \frac{\beta_{nQ}}{d_m^n} \right)^{-1} \end{aligned}$$

where coefficients β_{nP} and β_{nQ} account for the residual active and reactive power capability of node n.

Initially, all coefficients β are set to 1; they are then updated, at each computation step k, on the basis of the residual power capability measured at the previous computation step $k-1$, which is defined by the coefficients:

$$(17) \quad \begin{aligned} \alpha_{nP}(k) &= P_{n,MAX} / P_n(k-1) \\ \alpha_{nQ}(k) &= Q_{n,MAX} / Q_n(k-1) \end{aligned}$$

$P_{n,MAX}$ and $Q_{n,MAX}$ are the maximum active and reactive power that node n can deliver, while $P_n(k-1)$ and $Q_n(k-1)$ are the active and reactive power requested to node n at step $k-1$ (and that could be higher than the maximum values). Coefficients α_{nP} and α_{nQ} are as higher as the power capacity of node n exceeds the requested power. Coefficients β are then defined as:

$$(18) \quad \begin{aligned} \beta_{nP}(k) &= \beta_{nP}(k-1) * \alpha_{nP}(k) \\ \beta_{nQ}(k) &= \beta_{nQ}(k-1) * \alpha_{nQ}(k) \end{aligned}$$

This is a recursive formula by which coefficients β are updated, at each computation step, according to the excess power available at each active node in the previous step. This provides a fast adaptation of the power sharing criterion to load changes. In practice, coefficients β are constrained by:

$$(19) \quad 0 < \beta_{nPmin} < \beta_{nP} < 1, \quad 0 < \beta_{nQmin} < \beta_{nQ} < 1$$

to ensure that the ideal distance-based criterion (15.a) is applied in absence of EPP saturation, and to avoid that an EPP drops in the idle state ($\beta = 0$), which would keep stable according to (18).

Power sharing criterion (16) ensures dynamic saturation management, i.e., it distributes the load power demand among the various EPPs according to their actual power capability. In a practical implementation the computation step is limited by the load power calculation time (one half of line period at least) and by the communication delays between DERs. If possible, the system can be speeded up by defining a primary computation step h and a secondary computation step k. The rimary computation step h is the

sampling time at which the EPPs receive the load power requests and communicate with each other about the saturation limits $P_{n,MAX}$ and $Q_{n,MAX}$. This time step is limited by power measurement delay and communication bandwidth. Instead, secondary step k is the execution time of the recursive formula for saturation management, that can be executed in each EPP at very high speed (depending on the DSP/FPGA implementing local control).

As a final remark, in a practical implementation the active and reactive power deliverable by an EPP are constrained by the kVA rating of the inverter and by the actual power generated by the local energy source. The active power limit $P_{n,MAX}$ is computed first, then $Q_{n,MAX}$ is determined from the power rating of the EPP.

Control implementation

With the proposed technique, at each primary computation step every active node broadcasts the information on its residual power capability (coefficients α_{nP} and α_{nQ}) to all passive nodes and then collects their power requests, computed by (8). Thus, implementing the above cooperative control requires communication, data processing and measurement capability at every grid node, either active or passive. The communication speed is however limited and can be met by commercial power line communication (PLC) standards and protocols [10], like the modern PRIME (PoweRline Intelligent Metering Evolution) technology with OFDM modulation.

The distances between grid nodes, needed to implement algorithm (16), can be obtained by the DSO (Distribution System Operator). Otherwise, they can be estimated on-line by applying ranging techniques, e.g., those based on time-of-arrival (TOA) measurement [10].

Application Examples

The proposed application examples aim at validating the cooperative control approach by comparing its performance with the theoretical optimum control. The simulations are organized as follows: first, a phasorial simulation in Matlab is presented, to focus on the steady state performances of cooperative control. Then, the real-time simulation of a small network is considered, to analyze the control performance when all factors affecting the system dynamics are taken into account, i.e., power line impedances, inner control loops of the inverters, PLLs and delays caused by active and reactive power measurements.

1: Phasorial simulations

As a test bed for the analysis of cooperative control we consider first the single phase micro-grid of Fig.4, which refers to a typical residential settlement of 18 houses. Nine of them ($L_1 \dots L_9$) act as purely passive loads. Their rated power is:

$P_{N1} = 5kW @ \cos\varphi_{N1} = 0.91$ for loads L_1, L_2, L_6;

$P_{N2} = 2.5kW @ \cos\varphi_{N2} = 0.96$ for loads L_3, L_4, L_5;

$P_{N3} = 10kW @ \cos\varphi_{N3} = 0.80$ for the remaining loads.

The other nine houses ($G_1 \dots G_9$) are prosumers, with local power sources covering the local power demand and providing an extra-power capability to feed the passive loads. As stated in the theoretical analysis, loads and generators are modelled as AC current sources, and the simulation is developed in the phasorial domain. In this way the analysis results in a sequence of steady states in the phasorial domain, and this simplifies the assessment of the stationary and dynamic performance of the proposed controller under quasi-stationary operation, i.e. when the

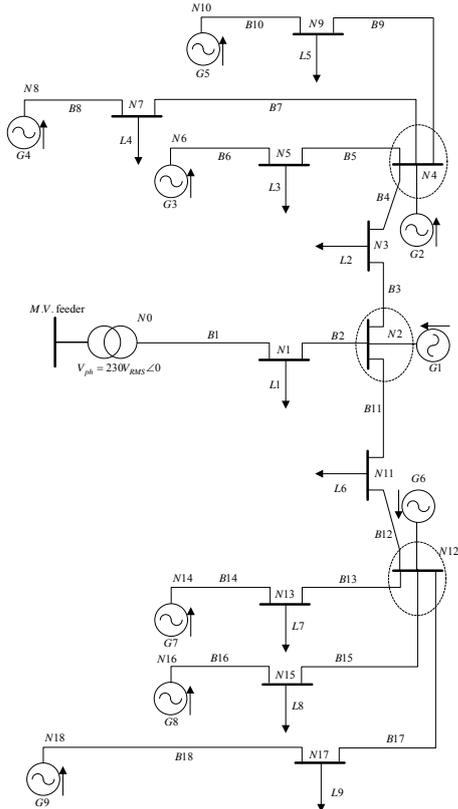system evolution is sufficiently slow as compared to the control response time.

Fig.4 Simulated microgrid

Table I: Prosumers available powers

G	Active Power (kW)	Apparent Power (kVA)
G_1, G_2, G_6	1	2
G_3, G_4, G_5	3	5
G_7, G_8, G_9	10	15

Table II: Bus lengths

Bus	Length (m)	Z (mΩ)
B1, B5, B6, B8, B9, B10, B11, B13, B14, B15, B16, B17	100	(16+j8)
B2, B3, B4, B12	50	(8+j4)
B7, B18	200	(32+j16)

For simplicity, we assume that the EPPs have full control on their active and reactive power up to the rated values. This means that every power source is tied to an energy storage device which stores the extra power generated and provides energy when needed. In the simulation, the control algorithm is adjourned sequentially in the active nodes, according to a token-ring approach. The token, in practice, is an enabling signal which allows only one EPP at a time to adjourn its power and current references. The other EPPs keep their current references unchanged, performing as constant current sources. In our example, the token moves cyclically from G_1 to G_9, and the duration of one iteration step corresponds to two line cycles.

Fig.5 shows the performance of cooperative control in terms of distribution loss. In particular Fig.5a shows the performance in case of purely distance-based sharing

criterion (15), while Fig.5b refers to the case of dynamic saturation management according to criterion (16). A load step variation of 50% is also considered to show the dynamic response of control.
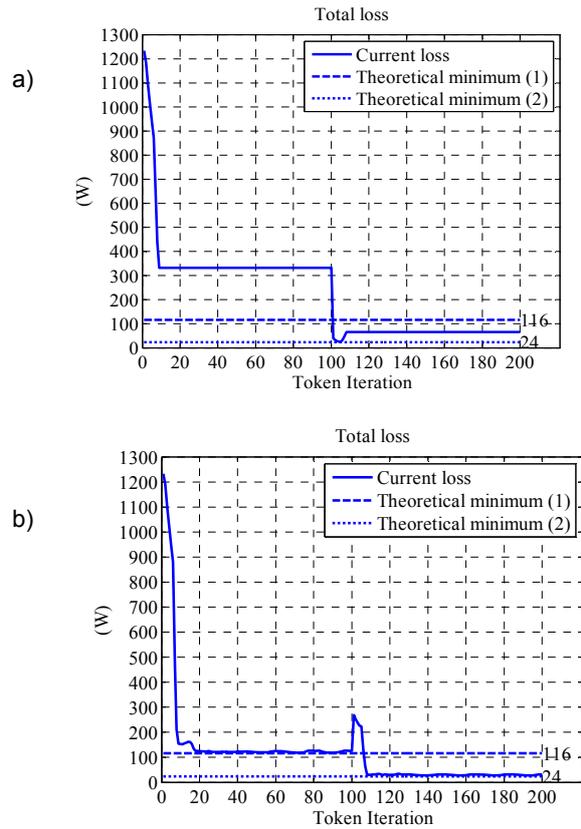

Fig.5 Distribution loss in the microgrid of Fig. 4, with EPPs driven by Cooperative Control

The distribution losses are plotted as a function of the token iteration, i.e., when the EPPs sequentially apply the control algorithm (15) or (16). Initially, all EPPs are idle and the full load power is provided by the utility at PCC. Correspondingly, the power losses are high (about 1200 W). Then, progressively, all EPPs begin injecting active and reactive power in the grid, and the distribution losses drop to a lower value (320 W in case *a*, and 120 W in case *b*). In case *a* the performance is worse than in case *b* since the EPP saturation is not managed, and the power requests that cannot be met by the active nodes are fulfilled by the utility at PCC. Instead, in case *b* such requests are shared among the active nodes nearby which still have some residual power capability.

Both cooperative control algorithms are compared with optimum control, showing similar performances. In particular, the minimum loss condition of case *1* (116W) refers to full-power absorption by the loads, while case *2* (24 W) refers to half-power absorption.

2: Real-time simulations
A deeper insight on the dynamic operation of cooperative control, focusing on the saturations management scheme, is given in this section, where a simple micro-grid including only two EPPs is considered. In this case, the EPP is fully modelled in a real-time platform, so as to test the control system in a real implementation scenario.

The considered set-up is shown in figure 6. The simple network with three branches, two EPPs and a single load, helps the understanding of the operation of the saturation management algorithm. Both EPPs include a current-

controlled inverter and they feed the load through branches B1 and B2. EPP1 is then connected to the main grid through branch BG. The distribution lines are made by cables with useful section S = 16mm² and parameter per unit of length r=2.4Ω/km and l=0.7mH/km. Table III gives the length and impedance of the branches of figure 6.

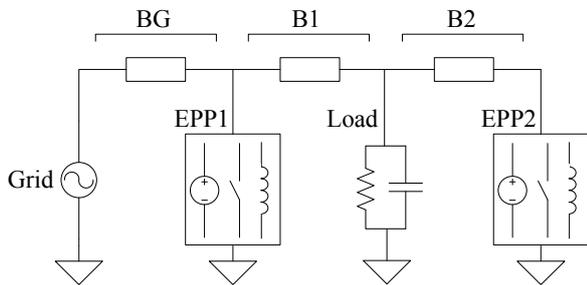Fig.6 Reduced microgrid implemented in the real-time platform

Table III: Bus lengths in Fig. 6

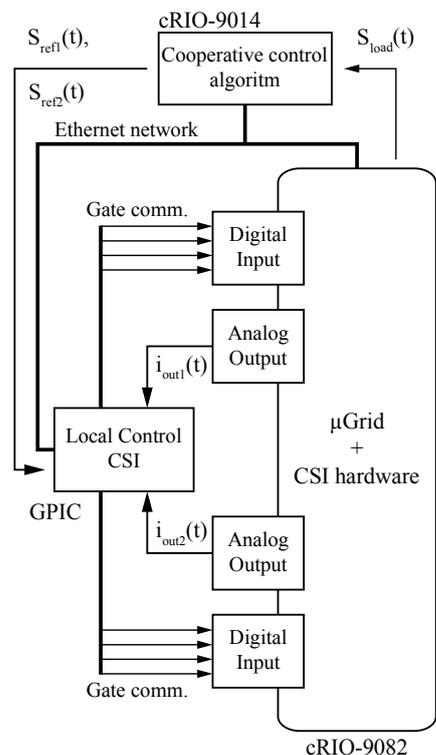| Bus	Length (m)	Z (mΩ)
BG	200	480+j 44
B1	100	240+j 22
B2	300	720+j 66

Fig.7 Architecture of the real-time platform

The complete models of the proposed setup have been implemented in NI LabVIEW to allow a real-time simulation of the grid and an HIL (Hardware In the Loop) validation of the local control of inverters. The system has been organized as follows: the microgrid model, including lines, load, main grid and the hardware part of the EPPs – i.e. the power switches and the output inductor of a full-bridge inverter - are implemented in a real-time processor; instead, the EPPs local control (including PLLs for synchronization, power measurements and current loops) is implemented in a separate general-purpose control board, that samples the outputs of the first processor and sends the commands to

the power switches; finally, a third processor emulates the communication architecture required by the cooperative control. The HIL is represented by the board containing the local control of the EPPs: in a real experimental setup the same board can seamlessly be used to control the EPPs, by only replacing the real-time simulated model of the grid and the inverters with the real hardware setup. For simplicity, in these simulations a single board has been used for two inverters, but in general each EPP could have its own local control board.

The architecture and organization of the real-time simulation platform is shown in figure 7. A cRIO-9082 and a cRIO-9014 National Instruments cRIO modules (compact Reconfigurable Input Output devices) and a National Instruments GPIC board (General Purpose Inverter Controller) are used to implement the architecture. Each of these devices include an FPGA core, a general-purpose processor, multiple digital and analog I/O ports and Ethernet communication capability.

Table IV Parameters for real-time simulation

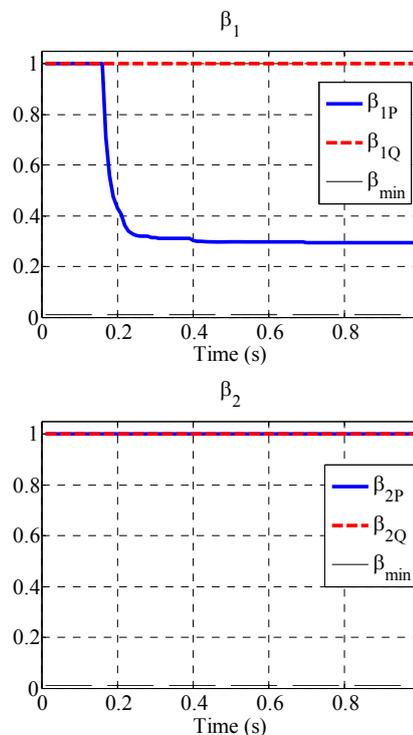| (P_{MAX1}, P_{MAX2}) /kW	(S_{MAX1}, S_{MAX2}) /kVA	$(β_{min1}, β_{min2})$
(2.0, 2.5)	(3.0, 3.0)	(0.01, 0.01)

Fig.8 Beta coefficients (18) for the microgid in Fig. 6 before and after the load step (synchronized with the step)

The model of the grid, the load and the hardware part of EPPs are simulated in real-time in the FPGA core of the cRIO-9082 module. The local current control of the two EPPs is implemented in the FPGA core of the GPIC board. The cooperative control algorithm runs in real-time in the general-purpose processor of the cRIO-9014 module. The communication between modules is provided via a dedicated Ethernet network, which accomplishes the periodic exchange of power measurements and commands.

Every nine line cycles (180ms) the module NI-9082 sends the measured power absorbed by the load to the NI cRIO-9014, which updates coefficients β and computes power references every ½ line cycle. The EPPs controller reads the computed power references for the two EPPs every

three grid cycles. As mentioned in the theoretical analysis of the saturation management scheme, the different execution rates of the cooperative control algorithm and the measurement of power quantities enables a tuning of the β coefficients dynamics, that becomes independent of the rate of update of the power references dispatched to the EPPs. The advantage is that the fast dynamic of the saturation management and the slower dynamic of the load variations become decoupled, ensuring the micro-grid to operate very close to minimum distribution loss condition.

The test case is further simplified by assuming that the load in Fig. 6 is purely resistive. The EPP power limits and the parameters of the saturation management are given in Table IV. The nominal line voltage is V_{G_RMS}=240V. The load is initially set to R_{L1}=38.4Ω, corresponding to P_{L1}=1.5kW. The load resistor is then suddenly reduced to R_{L2}=13.1Ω, causing the active power to step up to P_{L2}=4.4kW.The cooperative control updates the load power measurement every T_S=180ms, while the saturation management algorithm is executed at T_C=10ms. Moreover, the cooperative control implements also the condition of zero active power absorbed from the grid. This means that, within the power capability of the EPPs, the entire load power is shared among them by the distance criterion.
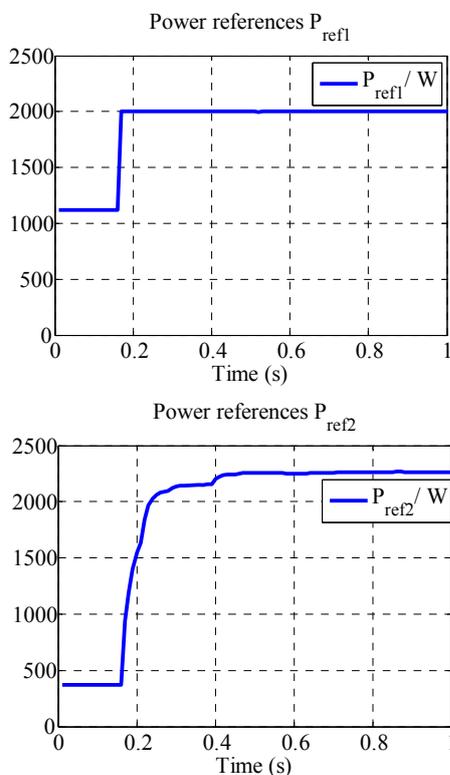

Fig.9 Active power injected by the EPPs in the microgid of Fig. 6 before and after the load step (synchronized with the step)

Therefore, from the distances in Table III, in absence of saturation, EPP1 is asked for ¾ of the load power, and EPP2 for the remaining ¼. This corresponds to the initial condition where the load absorbs P_{L1}=1.5kW, as reported in Fig. 8. At t=0 the load step occurs, but the detection only occurs in correspondence to the next sample, in the specific case at t_d=180ms. Fig. 10 shows the EPPs voltages before and after the load step, highlighting the sampling instants where the load power measurement is updated. Instead, Fig. 9 shows the active power generated by the EPPs, using the same time scale of Fig. 8. By comparing Fig. 8 and Fig.9 we note that after the load step the EPPs are no

longer able to maintain the ¾ - ¼ proportion in the load power sharing, because EPP1 should inject 3.3kW, that exceeds its power limit P_{MAX1}=2kW. For this reason, the saturation management automatically intervenes, and demands to EPP2 the missing portion of power, corresponding to 1.3kW. Hence, EPP2 injects 2.4kW instead of the power (1.1kW) that would be demanded in absence of saturation. The behaviour of coefficients β is reported in Fig. 8, showing how $β_{1P}$ is reduced until the load power sharing complies with the power limits of EPP1.

We conclude that the proposed saturation scheme is inherently stable, and guarantees fast adaption after load transients.
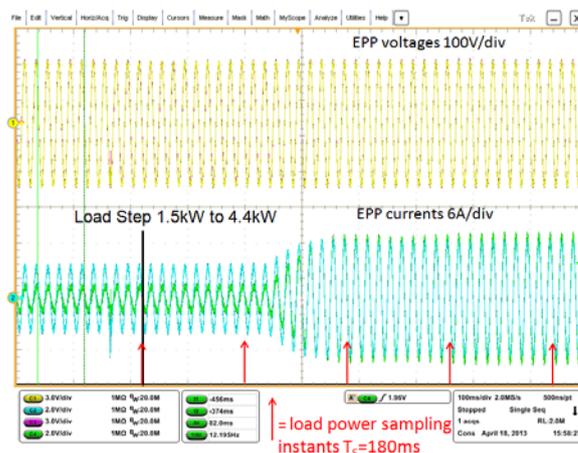

Fig.10 Voltages and currents of the EPPs as generated by the analog output modules of the real-time simulator

Conclusions

In the paper, three control techniques applicable to smart micro-grids have been discussed. The first method is based on an optimum control approach which requires full knowledge of the grid topology and parameters, relies on a centralized controller, and sets a benchmark for the achievable performance in terms of distribution efficiency and voltage stability. The second method is based on surround control, i.e., a distributed control technique which requires to know fewer network parameters and relies on narrowband communication among neighbour units. This control provides a significant reduction of distribution losses, full exploitation of distributed energy sources, and stabilization of grid voltage profiles, but requires tight time synchronization for measuring voltage and current phasors in the various units. The third method is the cooperative control, which only requires to measure and communicate power data among loads and distributed generators. Time synchronization is no longer needed, thus increasing the system robustness. Instead, the node-to-node distances must be known, or identified on-line by ranging techniques. The cooperative control also includes automatic adaptation to EPPs power limits, resulting in quasi-optimum operation of the micro-grid. Matlab/Simulink and real-time simulation results demonstrated the effectiveness of the proposed control technique.

REFERENCES
[1] Ipakchi and F. Albuyeh, "Grid of the future," Power and Energy Magazine, IEEE, vol. 7, no. 2, pp. 52 –62, march-april 2009.
[2] H. Farhangi, "The path of the smart grid," Power and Energy Magazine, IEEE, vol. 8, no. 1, pp. 18 –28, january-february 2010.
[3] D. Bakken, A. Bose, C. Hauser, D. Whitehead, and G. Zweigle, "Smart generation and transmission with coherent, real-time data," Proc. IEEE, vol. 99, no. 6, pp. 928 –951, june 2011.

[4] R. Anderson, A. Boulanger, W. Powell, and W. Scott, "Adaptive stochastic control for the smart grid," *Proc. IEEE*, vol. 99, no. 6, pp. 1098 –1115, june 2011.

[5] Dimeas and N. Hatziargyriou, "Operation of a multiagent system for microgrid control," *IEEE T. Power. Syst.*, vol. 20, no. 3, pp. 1447 – 1455, aug. 2005.

[6] J.-Y. Kim, J.-H. Jeon, S.-K. Kim, C. Cho, J. H. Park, H.-M. Kim, and K.-Y. Nam, "Cooperative control strategy of energy storage system and microsources for stabilizing the microgrid during islanded operation," *IEEE T. Power. Electr.*, vol. 25, no. 12, pp. 3037 –3048, dec. 2010.

[7] A. Mohsenian-Rad, V. Wong, J. Jatskevich, R. Schober, and A. Leon-Garcia, "Autonomous demand-side management based on game-theoretic energy consumption scheduling for the future smart grid," *IEEE T. Smart Grids*, vol. 1, no. 3, pp. 320 –331, dec. 2010.

[8] P.Tenti, D.Trombetti, P.Mattavelli, A. Costabeber: "Distribution Loss Minimization by Token Ring Control of Power Electronic Interfaces in Residential Micro-Grids", *IEEE International Symposium on Industrial Electronics* (ISIE 2010), Bari, July 2010.

[9] A. Costabeber, P. Tenti, and P. Mattavelli, "Distributed cooperative control of low-voltage residential microgrids," in *Power Electronics for Distributed Generation Systems (PEDG), 2012 3rd IEEE International Symposium on*, june 2012, pp. 457 –463.

[10] A. Costabeber, T. Erseghe, P. Tenti, S. Tomasin, and P. Mattavelli, "Optimization of micro-grid operation by dynamic grid mapping and token ring control," *Proceedings of the 2011-14th European Conference on Power Electronics and Applications (EPE 2011)*, 30 2011-sept. 1 2011, pp. 1 –10.

[11] R. Majumder, A. Ghosh, G. Ledwich, and F. Zare, "Power management and power flow control with back-to-back converters in a utility connected microgrid," IEEE T. Power. Syst., vol. 25, no. 2, pp. 821 –834, may 2010.

[12] Cagnano, E. De Tuglie, M. Liserre, and R. Mastromauro, "Online optimal reactive power control strategy of pv inverters," IEEE T. Ind. Electron., vol. 58, no. 10, pp. 4549 –4558, oct. 2011.

[13] K. Bhattacharya and J. Zhong, "Reactive power as an ancillary service," IEEE T. Power. Syst., vol. 16, no. 2, pp. 294 –300, may 2001.

[14] E. Serban and H. Serban, "A control strategy for a distributed power generation microgrid application with voltage- and current-controlled source converter," *IEEE T. Power. Electr.*, vol. 25, no. 12, pp. 2981 –2992, dec. 2010.

[15] J. Rocabert, G. Azevedo, A. Luna, J. Guerrero, J. Candela, and P. Rodriguez, "Intelligent connection agent for three-phase grid-connected microgrids," IEEE T. Power. Electr., vol. 26, no. 10, pp. 2993 –3005, oct. 2011.

[16] K. De Brabandere, B. Bolsens, J. Van den Keybus, A. Woyte, J. Driesen, R. Belmans, and K. Leuven, "A voltage and frequency droop control method for parallel inverters," in Power Electronics Specialists Conference, 2004. PESC 04. 2004 IEEE 35th Annual, vol. 4, 2004, pp. 2501 – 2507 Vol.4.

[17] J. Guerrero, J. Vasquez, J. Matas, L. de Vicuna, and M. Castilla, "Hierarchical control of droop-controlled ac and dc microgrids; a general approach toward standardization," IEEE T. Ind. Electron., vol. 58, no. 1, pp. 158 –172, jan. 2011.

[18] J. H. R. Enslin and P. J. M. Heskes, "Harmonic interaction between a large number of distributed power inverters and the distribution network," *IEEE Trans. Power Electronics*, pp. 1586–1593, 2004.

[19] J. De La Ree, V. Centeno, J. Thorp, and A. Phadke, "Synchronized phasor measurement applications in power systems," *IEEE T. Smart Grids*, vol. 1, no. 1, pp. 20 –27, june 2010.

[20] S. Galli, A. Scaglione, and Z. Wang, "For the grid and through the grid: The role of power line communications in the smart grid," *Proc. IEEE*, vol. 99, no. 6, pp. 998 –1027, june 2011.

[21] D. Dardari, A. Conti, U. Ferner, A. Giorgetti, and M. Win, "Ranging with ultrawide bandwidth signals in multipath environments," *Proc. IEEE*, vol. 97, no. 2, pp. 404 –426, feb. 2009.

[22] C. Smythe, "Iso 8802/5 token ring local-area networks," *Electronics Communication Engineering Journal*, vol. 11, no. 4, pp. 195 –207, aug 1999.

[23] L. Asiminoaei, R. Teodorescu, F. Blaabjerg, and U. Borup, "A Digital Controlled PV-Inverter With Grid Impedance Estimation for ENS Detection", *IEEE Trans. on Power Electronics*, pp. 1480-1490, 2005.

[24] M. Ciobotaru, R. Teodorescu and F. Blaabjerg, "On-line grid impedance estimation based on harmonic injection for grid-connected PV inverter*", 2007 IEEE Int. Symp. on Industrial Electronics*, pp. 2437-2442.

Authors: *Prof. Paolo Tenti, Dr. Alessandro Costabeber, Mr. Tommaso Caldognetto (PhD student), Department of Information Engineering University of Padova, Via Gradenigo 6/B, 35131 Padova Italy, E-mail paolo.tenti.@unipd.it; Prof. Paolo Mattavelli, Department of Management and Engineering, University of Padova at Vicenza, Stradella S. Nicola, 3 – 36100 Vicenza Italy, E-mail paolo.mattavelli@unipd.it;*

Prof. Paolo Tenti was born in Bolzano, Italy, in 1951. He received a degree with honors in Electrical Engineering from the University of Padova, Italy, in 1975. In 1979 he became a contract professor of Power Electronics, in 1981 a permanent researcher, and an associate professor in 1985. In 1990 he became full professor of Power Electronics at the University of Catania, Italy, and since 1991 he has been professor of Electronics at the University of Padova.

From 1991 to 2001 he was Member of the Executive Board of the IEEE Industry Applications Society, and in 1997 served as Society President. From 1996 he has been President of CREIVen, Research Center on Industrial Electronics, Italy. From 2001 to 2008 he was Director of the Department of Information Engineering of the University of Padova. From 2003 to 2008 he served as Chairman of the Council of Department Directors of the same University.

His main interests are in industrial electronics, power electronics, and electromagnetic compatibility. In these areas he published extensively and coordinated several research contracts at National and International level. In particular, he developed several contributions and some patents on the application of modern control theories to power electronics equipment for industrial and aircraft applications. More recently, he devoted his research activity to the growing field of distributed control of smart grids.

In 1997 Prof. Tenti was elevated to the IEEE Fellow grade and in 2000 was awarded the IEEE Millennium Medal.